

# Fourth-order perturbative extension of the singles-doubles coupled-cluster method

Andrei Derevianko\* and Erik D. Emmons

*Department of Physics, University of Nevada, Reno, Nevada 89557*

(Dated: November 11, 2018)

Fourth-order many-body corrections to matrix elements for atoms with one valence electron are derived. The obtained diagrams are classified using coupled-cluster-inspired separation into contributions from  $n$ -particle excitations from the lowest-order wavefunction. The complete set of fourth-order diagrams involves only connected single, double, and triple excitations and disconnected quadruple excitations. Approximately half of the fourth-order diagrams are *not* accounted for by the popular coupled-cluster method truncated at single and double excitations (CCSD). Explicit formulae are tabulated for the entire set of fourth-order diagrams missed by the CCSD method and its linearized version, i.e. contributions from connected triple and disconnected quadruple excitations. A partial summation scheme of the derived fourth-order contributions to all orders of perturbation theory is proposed.

PACS numbers: 31.15.Md, 31.15.Dv, 31.25.-v

## I. INTRODUCTION

Atomic tests of the low-energy electroweak sector of the standard model require both high-precision measurements and *ab initio* calculations of matching accuracy. The most precise measurement to date of parity violation in atoms has been carried by Wieman and co-workers using  $^{133}\text{Cs}$ . The accuracy of this experiment [1] is about 0.4%, while the relevant theoretical quantity is calculated with 0.4-1% uncertainty, depending on the authors's estimates [2, 3]. A keen interest in reducing the uncertainties is stimulated by a possible deviation of the resulting nuclear weak charge from the prediction of the standard model. This deviation was first reported in Ref. [2] and then scrutinized in Refs. [3]. Very recent analyses [3] of parity violation in  $^{133}\text{Cs}$  focused on effects of the Breit interaction, vacuum polarization, and neutron "skin", each contributing at the level of 0.2–0.6%. However, the effects of higher-order correlations beyond those considered in high-precision calculations by Dzuba et al. [4] and Blundell et al. [5] remain to be understood. Here we discuss in detail a possible extension to the method employed in Ref. [5].

The key to the 1% accuracy achieved in Refs. [4, 5] lies in the application of all-order methods based on relativistic many-body perturbation theory (MBPT). These techniques, although summing certain classes of MBPT diagrams to all orders of perturbation theory, still do not account for an infinite number of residual diagrams. It seems natural to augment a given all-order technique with some of the omitted diagrams so that the formalism is complete through a certain order of MBPT. To illustrate, the random-phase approximation (RPA) [6] fully recovers second order matrix elements but does not subsume all third-order diagrams. Among the omitted third-order contributions so called Brueckner-orbital diagrams

are known to be numerically as important as the RPA sequence (see, e.g., discussions in Refs. [7, 8]).

By the same virtue, certain diagrams starting from the fourth order of MBPT are missed in the popular coupled-cluster expansion [9, 10, 11] truncated at the single and double level of excitations (CCSD), although all third-order contributions are recovered [12]. It has been shown [13] that one of the subsets of the fourth-order terms missed by the CCSD method does contribute as much as a few per cent to Cs hyperfine-structure constants. At the same time, the considered subset leads to worse theory-experiment agreement for electric-dipole amplitudes [14]. We anticipate that a systematic accounting of *all* omitted fourth-order contributions to matrix elements in the CCSD method may lead to more accurate *ab initio* results. Here we derive such complementary fourth-order many-body contributions for matrix elements.

The paper is organized as follows. Basic starting formulas and notation of many-body perturbation theory (MBPT) are introduced in Section II. The linked-diagram expansion specialized to atoms with a single valence electron is discussed in Section III. The derived wave-functions through the third order of MBPT are discussed in Section IV and their relation to the truncated coupled-cluster method in Section V. Finally, the derived fourth-order corrections to matrix elements are tabulated in the Appendix and classification of the diagrams is given in Section VI. Fig. 5 summarizes the results of our work.

The fourth-order expressions presented here may be useful for an analysis of completeness of all-order methods and for designs of a hierarchy of next-generation approximations in atomic many-body calculations. As an example, we discuss all-order generalizations of the derived fourth-order contributions.

---

\*Electronic address: andrei@unr.edu

## II. PARTITIONING OF THE ATOMIC HAMILTONIAN

Here we briefly recap starting formulas of many-body perturbation theory (MBPT) for atoms with one valence electron. Our derivation in the fourth order of many-body perturbation theory may be considered as an extension of the work by Blundell et al. [15]. They presented formulas from first-, second-, and third-order perturbation theory. For the convenience of the reader we keep most of the original notation from Ref. [15].

The many-body Hamiltonian of an atomic system may be represented as

$$H = H_0 + V_I = \left( \sum_i h_{\text{nuc}}(\mathbf{r}_i) + \sum_i U_{\text{HF}}(\mathbf{r}_i) \right) + \left( \frac{1}{2} \sum_{i \neq j} \frac{1}{r_{ij}} - \sum_i U_{\text{HF}}(\mathbf{r}_i) \right), \quad (1)$$

where  $h_{\text{nuc}}$  includes the kinetic energy of an electron and its interaction with the nucleus,  $U_{\text{HF}}$  is the Hartree-Fock potential, and the last term represents the residual Coulomb interaction between electrons. The summations go over all electrons in the system. In MBPT the first part of the Hamiltonian is treated as the lowest-order Hamiltonian  $H_0$  and the residual Coulomb interaction as a perturbation  $V_I$ .

For atoms with one valence electron outside a closed-shell core the many-body wavefunction in the lowest order  $|\Psi_v^{(0)}\rangle$  is a Slater determinant constructed from core and valence single-particle orbitals  $u_k$  which satisfy

$$(h_{\text{nuc}}(\mathbf{r}) + U_{\text{HF}}(\mathbf{r})) u_k(\mathbf{r}) = \varepsilon_k u_k(\mathbf{r}). \quad (2)$$

The solutions of the above one-particle equation form a basis for application of the formalism of second quantization. In the second quantization the lowest-order Hamiltonian  $H_0$  and the perturbing residual Coulomb interaction  $V_I$  may be expressed as

$$H_0 = \sum_i \varepsilon_i a_i^\dagger a_i, \quad (3)$$

$$V_I = \frac{1}{2} \sum_{ijkl} g_{ijkl} a_i^\dagger a_j^\dagger a_l a_k - \sum_{ij} (U_{\text{HF}})_{ij} a_i^\dagger a_j, \quad (4)$$

where  $a_i^\dagger$  and  $a_i$  are creation and annihilation operators for a one-particle state  $i$ .

The Coulomb integral  $g_{ijkl}$  is conventionally defined as

$$g_{ijkl} = \int u_i^\dagger(\mathbf{r}) u_j^\dagger(\mathbf{r}') \frac{1}{|\mathbf{r} - \mathbf{r}'|} u_k(\mathbf{r}) u_l(\mathbf{r}') d^3r d^3r'. \quad (5)$$

The matrix elements of the Hartree-Fock potential may be expressed in terms of the antisymmetrized Coulomb integral  $\tilde{g}_{ijkl} = g_{ijkl} - g_{ijlk}$  as

$$(U_{\text{HF}})_{ij} = \sum_a \tilde{g}_{iaja}. \quad (6)$$

Here the summation is over core orbitals; this potential is the so-called frozen-core Hartree-Fock potential, i.e., first the core orbitals are calculated employing the self-consistent Hartree-Fock procedure and then the rest of the one-particle states are obtained using Eq. (6) without varying the determined core orbitals. Finally, in the language of second quantization the lowest-order wavefunction corresponds to  $|\Psi_v^{(0)}\rangle = a_v^\dagger |0_c\rangle$ , where  $v$  labels the one-particle state of the valence electron and the quasi-vacuum state  $|0_c\rangle$  describes the closed-shell core.

From a practical standpoint derivation of MBPT expressions is greatly simplified by the introduction of normal form of the operator products  $N[\dots]$  and by a subsequent application of the Wick theorem [11]. The notion of normal products arises from separation of one-particle states into two general categories - occupied in the quasi-vacuum state  $|0_c\rangle$  (i.e., core orbitals enumerated by letters  $a, b, c, d$ ) and complementary excited states (indices  $m, n, r, s$ ). Unspecified orbitals are labelled by indices  $i, j, k$ , and  $l$ . In this scheme the one-particle valence states  $v$  and  $w$  are classified as excited orbitals.

With the normal products

$$H_0 = E_c^{(0)} + \sum_i \varepsilon_i N[a_i^\dagger a_i] \quad (7)$$

and

$$V_I = E_c^{(1)} + \frac{1}{2} \sum_{ijkl} g_{ijkl} N[a_i^\dagger a_j^\dagger a_l a_k], \quad (8)$$

where  $E_c^{(0)} = \sum_a \varepsilon_a$  and  $E_c^{(1)} = -\frac{1}{2} \sum_a (U_{\text{HF}})_{aa}$ ; in the following discussion we omit these nonessential offset contributions.

It is worth noting that there is no one-body part of the perturbation  $V_I$  present in Eq. (8); this fact demonstrates the utility of the frozen-core Hartree-Fock potential in MBPT. In Ref. [15], the case of a model potential differing from  $U_{\text{HF}}$  was investigated explicitly and it was found that the number of resulting diagrams is substantially larger than in the Hartree-Fock case. Due to the very large number of diagrams in the fourth order, here we restrict our attention to the practically important frozen-core Hartree-Fock case.

## III. LINKED-DIAGRAM EXPANSION

We proceed to the derivation of many-body contributions to wavefunctions using the formalism of the generalized Bloch equation [11]. The Bloch equation is formulated for the wave operator  $\Omega_v$  which relates the exact wavefunction  $|\Psi_v\rangle$  to the lowest-order result  $|\Psi_v^{(0)}\rangle = a_v^\dagger |0_c\rangle$  as

$$|\Psi_v\rangle = \Omega_v |\Psi_v^{(0)}\rangle. \quad (9)$$

It should be noted that as defined, this exact wavefunction is not normalized, rather an intermediate normalization scheme  $\langle \Psi_v^{(0)} | \Psi_v \rangle = 1$  is employed in the formalism.

The exact correlation energy of the one-valence electron system is given by

$$\delta E = \langle \Psi_v^{(0)} | V_I \Omega_v | \Psi_v^{(0)} \rangle. \quad (10)$$

The wave-operator satisfies the linked-diagram version of the generalized Bloch equation

$$[\Omega_v, H_0] = \{Q V_I \Omega_v - (\Omega_v - 1) P V_I \Omega_v\}_{\text{linked}}, \quad (11)$$

where the operator  $P = |\Psi_v^{(0)}\rangle\langle\Psi_v^{(0)}|$  projects on the lowest-order wavefunction and  $Q = 1 - P$  is a complementary projection operator. The subscript “linked” in the above equation prescribes that all the *unlinked* Brueckner-Goldstone diagrams are to be discarded; a diagram is said to be unlinked if it contains a disconnected part with no free lines other than valence lines. Finally,  $[\Omega_v, H_0]$  is the commutator  $\Omega_v H_0 - H_0 \Omega_v$ .

The traditional Rayleigh-Schrödinger perturbation theory is recovered from the Bloch equation (11) by expanding the wave operator in powers of the residual interaction  $V_I$ ,  $\Omega_v = \sum_{n=0} \Omega_v^{(n)}$ . The resulting recursive relation is [11]

$$[\Omega_v^{(n)}, H_0] = \left\{ Q V_I \Omega_v^{(n-1)} - \sum_{m=1}^{n-1} \Omega_v^{(n-m)} P V_I \Omega_v^{(m-1)} \right\}_{\text{linked}}. \quad (12)$$

Here the iterations start with  $\Omega_v^{(0)} = 1$ . A corresponding perturbative expansion of correlation energy reads

$$\delta E_v = \sum_{n=1} \delta E_v^{(n)} = \sum_{n=1} \langle \Psi_v^{(0)} | V_I \Omega_v^{(n-1)} | \Psi_v^{(0)} \rangle. \quad (13)$$

The last term on the r.h.s. of Eq.(12) gives rise to so-called “folded” or “backward” diagrams [11]. Instead of calculating the explicit contributions of folded diagrams we use an all-order approach which incorporates their effect in modified energy denominators. Such a reformulation allows for a direct link to the coupled-cluster method outlined in Section V. The exact wave-operator  $\Omega_v$  may be separated into valence and core parts,  $\Omega_v = \Omega_v^{\text{val}} + \Omega_v^{\text{core}}$ , the  $\Omega_v^{\text{val}}$  part promoting a valence electron from the  $|\Psi_v^{(0)}\rangle$  determinant into an excited state.  $\Omega_v^{\text{core}}$ , describing excitations of core electrons, does not depend on any particular valence state. Similarly, the correlation contribution to the total energy of the system  $\delta E_v$  may be broken into corrections to the energies of valence and core electrons,  $\delta E_v = \delta E_v^{\text{val}} + \delta E_v^{\text{core}}$ .

Suppose that the valence removal energy  $\varepsilon_v + \delta E_v^{\text{val}}$  is known at the desired order of perturbation theory (e.g., from coupled-cluster calculations) or from experiment. Projecting the original Bloch equation (11) onto  $|\Psi_v^{(0)}\rangle$  and using the definition of the projection operator  $P$  together with Eq. (10) for the correlation energy, one may show that

$$[\Omega_v, H_0] |\Psi_v^{(0)}\rangle = \{Q V_I \Omega_v\}_{\text{linked}} |\Psi_v^{(0)}\rangle - \delta E_v^{\text{val}} \Omega_v^{\text{val}} |\Psi_v^{(0)}\rangle.$$

Notice that the last term is represented by a product of two valence contributions, since all other terms produce unlinked diagrams. Expanding the commutator and explicitly breaking the term  $\{Q V_I \Omega_v\}_{\text{linked}}$  into valence and core contributions we arrive at

$$\begin{aligned} (\varepsilon_v + \delta E_v^{\text{val}} - H_0) \Omega_v^{\text{val}} |\Psi_v^{(0)}\rangle &= (\{Q V_I \Omega_v\}_{\text{linked}})^{\text{val}} |\Psi_v^{(0)}\rangle, \\ (\varepsilon_v - H_0) \Omega_v^{\text{core}} |\Psi_v^{(0)}\rangle &= (\{Q V_I \Omega_v\}_{\text{linked}})^{\text{core}} |\Psi_v^{(0)}\rangle. \end{aligned}$$

Accounting for the folded diagrams in this way leads to an additional shift  $\delta E_v^{\text{val}}$  in energy denominators of diagrams for the valence part of the wave operator  $\Omega_v^{\text{val}}$ . Mnemonically, every occurrence of the Hartree-Fock energy of the valence electron  $\varepsilon_v$  in the energy denominators has to be replaced by the total removal energy  $\varepsilon_v + \delta E_v^{\text{val}}$ , since  $(\varepsilon_v - H_0) \Omega_v^{\text{core}} |\Psi_v^{(0)}\rangle$  simplifies to  $(-H_0) \Omega_v^{\text{core}} |0_c\rangle$ . Keeping this rule in mind, we may combine the above equations

$$(\varepsilon_v + (\delta E_v^{\text{val}}) - H_0) \Omega_v |\Psi_v^{(0)}\rangle = \{Q V_I \Omega_v\}_{\text{linked}} |\Psi_v^{(0)}\rangle, \quad (14)$$

where  $(\delta E_v^{\text{val}})$  means that the  $\delta E_v^{\text{val}}$  correction should be included for the valence diagrams of  $\Omega_v$  and discarded otherwise.

We expand the wave operator in powers of the residual electron-electron interaction  $V_I$ ,  $\Omega_v = \sum_{n=0} \Omega_v^{(n)}$  and obtain

$$(\varepsilon_v + (\delta E_v^{\text{val}}) - H_0) \Omega_v^{(n+1)} |\Psi_v^{(0)}\rangle = \{Q V_I \Omega_v^{(n)}\}_{\text{linked}} |\Psi_v^{(0)}\rangle,$$

with  $\Omega_v^{(0)} = 1$ . This equation may be interpreted as a linked-diagram version of the Brillouin-Wigner perturbation theory for atoms with one valence electron outside a closed core. Introducing the resolvent operator

$$R_v = (H_0 - [\varepsilon_v + (\delta E_v^{\text{val}})])^{-1}, \quad (15)$$

we obtain (with  $|\Psi_v^{(n)}\rangle \equiv \Omega_v^{(n)} |\Psi_v^{(0)}\rangle$ )

$$\begin{aligned} |\Psi_v^{(n)}\rangle &= -R_v \{Q V_I |\Psi_v^{(n-1)}\rangle\}_{\text{linked}} = \\ &= (-1)^n (\{R_v Q V_I\}_{\text{linked}})^n |\Psi_v^{(0)}\rangle. \end{aligned}$$

From this recursion relation we may generate corrections to wave functions at any given order of perturbation theory. In practice, the derivation is rather tedious and error-prone. We employed the symbolic algebra system Mathematica [16] to derive the expressions presented in this work.

#### IV. WAVEFUNCTIONS THROUGH THE THIRD ORDER OF MBPT

For the derivation of fourth-order matrix elements one requires contributions to wavefunctions through the third

order. Expressions for  $|\Psi_v^{(n)}\rangle = \Omega_v^{(n)}|\Psi_v^{(0)}\rangle$  through the second order may be found in Ref. [15]. Although we fully derived  $|\Psi_v^{(3)}\rangle$ , to keep the manuscript to a manageable size, we present below only a qualitative discussion of the third-order correction to the wave-function.

The contributions to the wave operator  $\Omega_v$  are conventionally classified by the number of excitations from a reference determinant  $|\Psi_v^{(0)}\rangle = a_v^\dagger|0_c\rangle$ . The first-order result,  $\Omega_v^{(1)}$ , contains only double excitations drawn in Fig. 1. We may distinguish between valence and core excitations. The former promote the valence electron to an excited state ( $\Omega_v^{\text{val}}$ ) and the latter do not modify the state of valence electron ( $\Omega_v^{\text{core}}$ ). With such a classification the diagram Fig. 1(a) represents core doubles  $D_c$  and Fig. 1(b) valence doubles  $D_v$ .

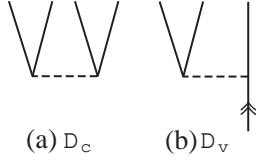


FIG. 1: Brueckner-Goldstone diagrams for the first-order wave operator  $\Omega_v^{(1)}$ . Horizontal dashed lines represent residual Coulomb interaction between electrons and vertical lines are particle/hole lines. The valence line is marked by double arrow.

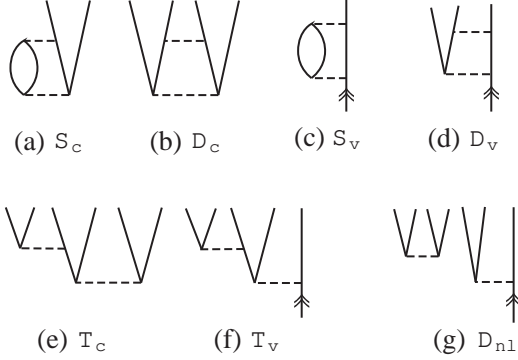


FIG. 2: Sample contributions to the second-order wave operator  $\Omega_v^{(2)}$ .

The second-order operator  $\Omega_v^{(2)}$  contains excitations up to quadruples. Examples of contributions to  $\Omega_v^{(2)}$  are drawn in Fig. 2. Diagrams 2(a) and (b) represent some of the second-order core singles and doubles. Valence singles and doubles are drawn in Fig. 2(c) and (d) respectively. Diagrams 2(e) and (f) represent core and valence triple excitations, and (g) — disconnected quadruple excitations. A sum of the the quadruple contribution 2(g) and a similar diagram with the order of the two interactions reversed is known to factorize into a normal product of double excitations [11]; this is demonstrated in Fig. 3.

We classify the disconnected quadruple contribution 2(g) as a nonlinear contribution of double excitations to wave-functions.

$$\text{Diagram 2(g)} + \text{Diagram 2(g) with reversed interactions} = N[\text{Diagram 2(a)} \otimes \text{Diagram 2(c)}]$$

FIG. 3: A sum of the the quadruple contribution Fig. 2(g) and a similar diagram with the order of two interactions reversed factorizes into a normal product of double excitations. On the r.h.s. the energy denominators are to be evaluated separately.

Several contributions to the third-order wave-operator  $\Omega_v^{(3)}$  are shown in Fig. 4. Single and double excitations shown in Fig. 4(a–e) contain intermediate triple excitations. Diagram 4(f) is due to intermediate second-order quadruple excitation. For the sake of comparison with the coupled-cluster method we classify diagram 4(a) as the effect of core triples on core singles ( $S_c[T_c]$ ), (b) as modification of core doubles by core triples ( $D_c[T_c]$ ), (c) as the effect of core triples on valence doubles ( $D_v[T_c]$ ), and (d) and (e) as the effect of valence triples on valence singles and doubles ( $S_v[T_v]$  and  $D_v[T_v]$ ). Finally, diagram 4(f) may be classified as an effect of nonlinear doubles, Fig. 2(g), on valence doubles ( $D_v[D_{nl}]$ ). It is worth noting that the third-order wavefunction contains connected quadruple excitations and some additional disconnected excitations; these corrections do not contribute to the fourth-order matrix elements.

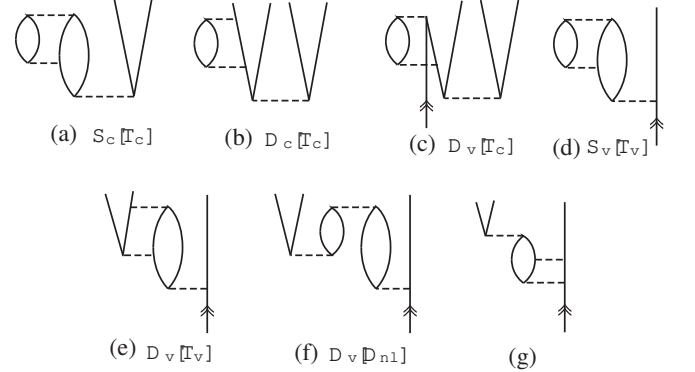


FIG. 4: Representative diagrams for the third-order wave operator  $\Omega_v^{(3)}$ .

## V. COUPLED-CLUSTER METHOD

The coupled-cluster (CC) formalism [9, 10] is widely employed in atomic and nuclear physics, and quantum chemistry [17]. The main goal of the present work is to identify fourth-order contributions to matrix elements

not included in the truncated singles-doubles coupled-cluster method, and here we review the relevant features of this all-order approach.

The key point of the coupled-cluster method is the introduction of an exponential ansatz for the wave operator [11]

$$\Omega = N[\exp(S)] = 1 + S + \frac{1}{2!}N[S^2] + \dots \quad (16)$$

The cluster operator  $S = \Omega_{\text{conn}}$  is expressed in terms of *connected* diagrams of the wave operator  $\Omega$ , an example of disconnected diagram being Fig. 2(g). The operator  $S$  is naturally broken into cluster operators  $S_n$  combining  $n$  simultaneous excitations from the reference state  $|\Psi_v^{(0)}\rangle$  in all orders of perturbation theory.

Let us specialize the general formalism of Ref. [11] to the case of atoms with one valence electron. A set of coupled equations for the cluster operators may be found by considering connected diagrams on both sides of the modified Bloch equation (14)

$$(\varepsilon_v + (\delta E_v^{\text{val}}) - H_0) S_n = \{Q V_I \Omega_v\}_{\text{conn},n}, \quad (17)$$

where  $\delta E_v$  is determined by Eq. (10) and wave operator  $\Omega_v$  by Eq. (16). Term  $(\delta E_v^{\text{val}})$  accounts for folded diagrams; it is to be omitted for core and included for valence clusters. Successive iterations of such all-order equations explicitly recover order-by-order MBPT contributions to the wave operator discussed in the previous sections.

In most applications the full operator  $S$  is truncated at single and double excitations (CCSD method). For univalent atoms the CCSD parameterization may be represented as

$$\begin{aligned} S^{\text{SD}} = S_1 + S_2 = & \sum_{ma} \rho_{ma} a_m^\dagger a_a + \frac{1}{2} \sum_{mnab} \rho_{mnab} a_m^\dagger a_n^\dagger a_b a_a + \\ & \sum_{m \neq v} \rho_{mv} a_m^\dagger a_v + \sum_{mna} \rho_{mnva} a_m^\dagger a_n^\dagger a_a a_v, \end{aligned} \quad (18)$$

where the first two terms represent single and double excitations of core electrons and the remaining contributions are valence singles and doubles.

It is worth emphasizing that the CCSD method is an all-order method. For example, first-, second- and third-order diagrams Fig. 1(b), Fig. 2(d), and Fig. 4(g) are encapsulated in the valence doubles term  $\sum_{mna} \rho_{mnva} a_m^\dagger a_n^\dagger a_a a_v$ . Similarly, the CCSD method accounts for all single and double excitations (both core and valence) shown in Figs. 1 and 2. At the same time connected triple and higher-rank excitations are not accounted for by the CCSD method, examples being Fig. 2(e),(f) and Fig. 4 (a-e). Although diagrams Fig. 4 (a-e) are nominally single or double excitations, they contain connected triples as intermediate excitations and are not included in the sequence of CCSD diagrams.

A *linearized* version of the CCSD method (LCCSD) is a further simplification of a hierarchy of all-order methods based on the coupled-cluster formalism. In this approximation  $\Omega_v^{\text{LCCSD}} \equiv 1 + S^{\text{SD}}$ . For alkali-metal atoms the LCCSD method was employed in Refs. [12, 13, 14, 18]. Compared to the full CCSD approximation the linearized version misses a subset of diagrams shown in Fig. 2(g) and 4(f).

To reiterate, connected triple excitations and disconnected quadruple excitations first appear in the second order wavefunctions. In order to systematically extend the CCSD method one has to investigate the contributions of connected triple excitations and the role of non-linear contributions for the linearized CCSD approximation.

## VI. MATRIX ELEMENTS

We investigate the fourth-order corrections to matrix element of a one particle operator  $Z = \sum_i z(\mathbf{r}_i)$ . In second quantization

$$Z = \sum_{ij} z_{ij} a_i^\dagger a_j = \sum_a z_{aa} + \sum_{ij} z_{ij} N[a_i^\dagger a_j], \quad (19)$$

where  $N[\dots]$  denotes normal form of operator products. We are mainly interested in matrix elements of non-scalar operators, like electromagnetic transition amplitudes or pseudo-scalar operators, like the electroweak interaction. For such operators the contribution from the zero-body term  $\sum_a z_{aa}$  vanishes and we disregard it in the following discussion.

The exact matrix element between two valence states  $w$  and  $v$  is given by

$$M_{wv} = \frac{Z_{wv}}{\sqrt{N_v N_w}} = \frac{\langle 0_c | a_w \Omega_w^\dagger Z \Omega_v a_v^\dagger | 0_c \rangle}{\sqrt{N_v N_w}}, \quad (20)$$

where  $\Omega_w$  and  $\Omega_v$  correspond to wave operators for valence states  $w$  and  $v$  respectively. Since the wave-operators were derived using the intermediate normalization scheme, we introduced normalization factors

$$N_v = \langle \Psi_v^{(0)} | \Omega_v^\dagger \Omega_v | \Psi_v^{(0)} \rangle$$

in the definition of matrix element.

Blundell et al. [12] have demonstrated that disconnected diagrams in the perturbative expansion of the numerator and the denominator of Eq. (20) cancel. Their final expression for the exact matrix element reads

$$M_{wv} = \delta_{wv} (Z^{\text{core}})_{\text{conn}} + \frac{(Z_{wv}^{\text{val}})_{\text{conn}}}{\{[1 + (N_v^{\text{val}})_{\text{conn}}][1 + (N_w^{\text{val}})_{\text{conn}}]\}^{1/2}}, \quad (21)$$

where

$$Z^{\text{core}} \equiv \langle 0_c | \Omega_w^\dagger Z \Omega_v | 0_c \rangle = \langle 0_c | (\Omega^{\text{core}})^\dagger Z \Omega^{\text{core}} | 0_c \rangle$$

and the remaining contributions of  $Z_{wv} = \langle 0_c | a_w \Omega_w^\dagger Z \Omega_v a_v^\dagger | 0_c \rangle$  are grouped into the valence part  $Z_{wv}^{\text{val}}$ . The diagrams of  $Z_{wv}^{\text{val}}$  explicitly depend on valence indices  $w$  and  $v$ . The valence part of the normalization factor  $N_v^{\text{val}}$  is defined in a similar fashion. The core contribution  $Z^{\text{core}}$  vanishes for non-scalar (and pseudo-scalar) operators and we disregard  $Z^{\text{core}}$  in the following discussion. Notice that all the diagrams in Eq. (21) must be rigorously connected as emphasized by subscripts “conn”.

The formulas for contributions to matrix elements through the third-order of MBPT were presented in Ref. [15]. The linearized coupled-cluster approach truncated at single and double excitations (LCCSD) fully recovers the matrix elements through the third order [12]. Here we investigate the contributions at the fourth order missed by the LCCSD method.

To derive the fourth-order correction to a matrix element, we expand the matrix element and normalization factors into powers of the residual Coulomb interaction  $Z_{wv} = \sum_{k=1} Z_{wv}^{(k)}$ ,  $N_v = \sum_{k=0} N_v^{(k)}$ . Further, we employ the all-order result, Eq. (21), and expand the normalization denominator into series. The result is

$$M_{wv}^{(4)} = \left\{ \langle \Psi_w^{(1)} | Z | \Psi_v^{(2)} \rangle + \langle \Psi_w^{(0)} | Z | \Psi_v^{(3)} \rangle + \langle \Psi_w^{(2)} | Z | \Psi_v^{(1)} \rangle + \langle \Psi_w^{(3)} | Z | \Psi_v^{(0)} \rangle \right\}_{\text{val,conn}} + Z_{wv, \text{norm}}^{(4)}, \quad (22)$$

where only connected valence contributions are to be kept. The normalization correction is given by

$$Z_{wv, \text{norm}}^{(4)} = -\frac{1}{2} \left( N_v^{(2)} + N_w^{(2)} \right)_{\text{val,conn}} \left( Z_{wv}^{(2)} \right)_{\text{val,conn}} + -\frac{1}{2} \left( N_v^{(3)} + N_w^{(3)} \right)_{\text{val,conn}} z_{wv}, \quad (23)$$

where we used that  $N_v^{(1)} = 0$  and  $Z_{wv}^{(1)} \equiv z_{wv}$ , the matrix element in the Hartree-Fock approximation.

As we proceed to the derivation of the fourth-order diagrams we notice that the second line of Eq. (22) is the hermitian conjugate of the first line with a swap of valence indexes  $w$  and  $v$ . This observation allows us to consider only half of the diagrams since in numerical evaluation the conjugated terms do not require additional programming efforts.

## VII. DISCUSSION OF FOURTH-ORDER DIAGRAMS

We fully derived the fourth-order correction to matrix elements using Wick theorem. A set of simplification rules was implemented with the symbolic algebra system *Mathematica* [16]. Excluding the normalization correction and folded diagrams, the resulting number of diagrams in the fourth order is 262. We counted both direct and all possible exchange forms of a given diagram

as a single contribution. We excluded hermitian conjugated terms from the counting procedure. The linearized coupled cluster approach, truncated at single and double excitations (LCCSD) recovers approximately half of the fourth-order contributions. The remaining diagrams are due to triple excitations (128 terms) and nonlinear contribution of double excitations (14 terms). Explicit expressions for these complementary contributions are given in the Appendix.

We break all fourth-order contributions complementary to the LCCSD subset of diagrams into nine classes:

$$\begin{aligned} \left( M_{wv}^{(4)} \right)_{\text{non-LCCSD}} &= Z_{1 \times 2}(T_v) + Z_{1 \times 2}(T_c) + \\ &Z_{0 \times 3}(S_v[T_v]) + Z_{0 \times 3}(D_v[T_v]) + \\ &Z_{0 \times 3}(S_c[T_c]) + Z_{0 \times 3}(D_v[T_c]) + \\ &Z_{1 \times 2}(D_{nl}) + Z_{0 \times 3}(D_{nl}) + Z_{\text{norm}}(T_v). \end{aligned} \quad (24)$$

The representative diagrams for each class of contributions are shown in Fig. 5. Here the diagrams  $Z_{1 \times 2}(\dots)$  arise from evaluation of expression  $\langle \Psi_w^{(1)} | Z | \Psi_v^{(2)} \rangle$  and its hermitian conjugate with a swap of valence labels  $w$  and  $v$ . Similarly  $Z_{0 \times 3}(\dots)$  terms are generated from  $\langle \Psi_w^{(0)} | Z | \Psi_v^{(3)} \rangle + \text{c.c.}$  Finally  $Z_{\text{norm}}(\dots)$  are due to normalization correction, Eq. (23). Further, we classify the diagrams by the presence of core triples ( $T_c$ ) or valence triples ( $T_v$ ). For  $Z_{0 \times 3}(\dots)$  terms triple excitations occur as an intermediate contribution (see Fig. 4) and we distinguish the effect of triples on lower-rank excitations, e.g.  $D_v[T_c]$  is the effect of core triples on valence doubles. Finally, the diagrams marked  $D_{nl}$  are due to the effect of disconnected quadruple excitations. These diagrams may be simplified to a direct product of double excitations, as demonstrated in Fig. 3.

The introduced classes of diagrams are illustrated in Fig. 5. The numbers of contributions in each class are also given in that figure. Let us make some observations. First of all, none of the diagrams contain computationally intensive Coulomb integrals involving four particle states, e.g.,  $g_{mnr s}$ . We also notice the absence of term  $D_c[T_c]$ , i.e., the effects of core triples on core double excitations. The core triples also do not contribute to the normalization correction. All these simplifications may lead to a design of an efficient numerical evaluation scheme.

The dominant number of diagrams is due to valence triple excitations, the set  $Z_{1 \times 2}(T_v)$  accounting for 44 and the set  $Z_{0 \times 3}(D_v[T_v])$  for 36 contributions. We further distinguish second-order triples  $T$  by the nature of the orbital line connecting upper and lower interactions  $T = T^p + T^h$ ,  $T^p$  standing for a particle line and  $T^h$  for a hole line as illustrated in Fig. 6. Such a separation is motivated by considerations of computational complexity: the  $T^h$  diagram, involving summation over a small number of core states, may be calculated much faster than a similar  $T^p$  contribution. We write

$$\begin{aligned} Z_{1 \times 2}(T_v) &= Z_{1 \times 2}(T_v^p) + Z_{1 \times 2}(T_v^h), \\ Z_{0 \times 3}(D_v[T_v]) &= Z_{0 \times 3}(D_v[T_v^p]) + Z_{0 \times 3}(D_v[T_v^h]). \end{aligned}$$

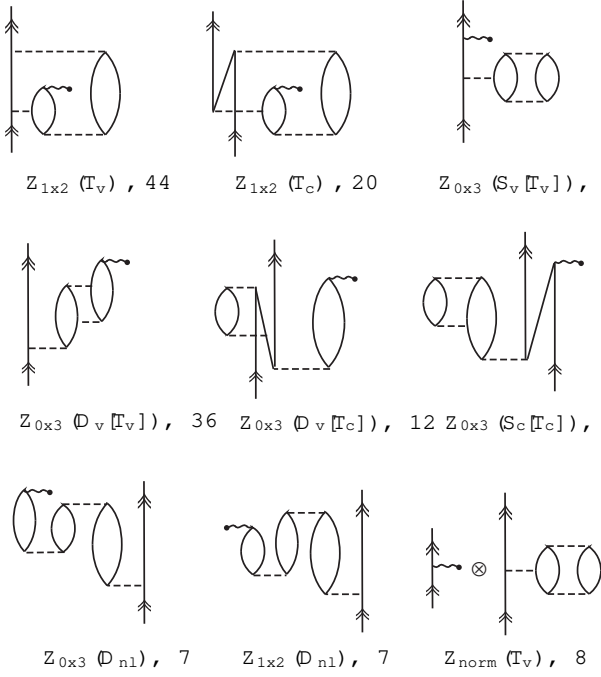


FIG. 5: Sample fourth-order diagrams involving triple excitations and non-linear coupled-cluster contributions. The one-particle matrix element is denoted by a wavy horizontal line. See the explanation in the text for diagram classification. The number of contributions for each class of diagrams is also shown; direct, all possible exchange, and the conjugated graphs of a given diagram were counted as a single contribution.

The formulas in the Appendix are grouped according to this scheme.

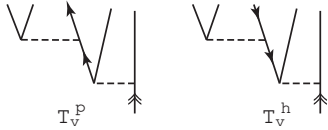


FIG. 6: Separation of triple excitations based on a nature of an orbital line connecting upper and lower interactions.  $T_v^p$  diagram involves particle line and  $T_v^h$  a hole line. Similar separation may be carried out for core triples.

The effect of triples on *single* excitations in  $\Omega_v^{(3)}$ , such as diagrams 4(a) and (d), has been treated previously in Refs. [13, 14]. Corresponding contributions to  $M_{vv}^{(4)}$ ,  $Z_{0 \times 3}(S_v[T_v])$  and  $Z_{0 \times 3}(S_c[T_c])$  are shown in Fig. 5. It was found that this effect contributes as much as 5% to hyperfine-structure constants in Cs, and brings the *ab initio* calculations into 0.5% agreement with experiment. At the same time the experiment-theory agreement becomes worse for electric-dipole matrix elements when the  $S[T]$  effect is included. To fully understand the role of triple excitations it is important to investigate all the enumerated effects on triple excitations, i.e. effect of

triples on valence doubles, direct contribution of triple excitations to matrix elements entering  $Z_{1 \times 2}$ , and also the normalization correction due to valence triple excitations.

The *linearized* coupled-cluster method (LCCSD) [12, 13, 14, 18] additionally disregards nonlinear terms in the coupled-cluster expansion. Therefore contributions to  $\Omega_v^{(3)}$  similar to one shown in Fig. 4(f) are omitted. These nonlinear terms lead to additional corrections  $Z_{0 \times 3}(D_{nl})$ . A similar effect omitted in the LCCSD approach is a direct contribution of disconnected double excitations to matrix elements represented by the diagrams of  $Z_{1 \times 2}(D_{nl})$  class. It is worth noting that consideration of the nonlinear contributions is key for accounting for the full set of random-phase-approximation diagrams with the CCSD method.

We further notice that in the framework of traditional Rayleigh-Schrödinger perturbation theory there are also contributions from so-called folded diagrams, as discussed in Section III. These folded diagrams originate from the second-order valence energy correction (the first-order correction is zero in the frozen-core Hartree-Fock basis). Since both the CCSD method and its linearized version fully recover the second order energies [12], in our approach we have omitted contributions of the folded diagrams.

Finally, we would like to comment on a possible all-order extension of the derived fourth-order contributions. Ideally, the entire fourth order set of diagrams would be recovered by fully treating the triple and nonlinear double excitations within the traditional coupled-cluster approach. However, at the present state of computer technology such a full treatment hardly seems feasible in relativistic calculations. At the same time the coupled-cluster expansion truncated at the single and double excitations (CCSD method) presents an attractive starting point. The triple excitations may be treated semi-perturbatively, i.e., the triple excitations are replaced by a combination of “bare” Coulomb interaction and an all-order CCSD double excitation [13].

The following modifications of the CCSD method should be made to partially sum the derived diagrams to all orders of perturbation theory: (i) Four classes of the derived diagrams ( $Z_{0 \times 3}(S_v[T_v])$ ,  $Z_{0 \times 3}(D_v[T_v])$ ,  $Z_{0 \times 3}(S_c[T_c])$ ,  $Z_{0 \times 3}(D_v[T_c])$ ) may be accounted for by amending the traditional CCSD equations with a semi-perturbative contribution of triple excitations. Two of the desired modifications,  $S_v[T_v]$  and  $S_c[T_c]$ , were considered previously in Ref. [13, 14]. (ii) In the diagrams  $Z_{1 \times 2}(T_v)$ ,  $Z_{1 \times 2}(T_c)$ , and  $Z_{\text{norm}}(T_v)$  the bottom and the upper (closing) Coulomb interactions should be replaced by all-order double excitation amplitudes. This generalization follows from considering the relevant contributions in the coupled-cluster method. (iii) In the  $Z_{1 \times 2}(D_{nl})$  diagrams all the Coulomb interactions should be replaced by all-order double excitation amplitudes. (iv) The linearized coupled-cluster expansions should include terms nonlinear in double ex-

citations to recover the diagrams  $Z_{0 \times 3}(D_{nl})$  in all-order fashion.

### VIII. CONCLUSION

An improvement of the accuracy of *ab initio* Coulomb-correlated calculations is necessitated by the latest experimental and theoretical progress in studies of parity violation in alkali-metal atoms. Such improvement may possibly be achieved by augmenting powerful all-order techniques by contributions missed in a given order of many-body perturbation theory. We derived and analyzed the entire set of fourth-order many-body diagrams for a one-particle operator.

We highlighted the fourth-order contributions omitted in the popular coupled-cluster approach truncated at single and double excitations (CCSD). To recover the full set of fourth-order diagrams one should additionally consider the effect of triple excitations. In addition, the linearized version of CCSD should be augmented by nonlinear contributions of double excitations. We presented explicit formulas for such complementary contributions in the Appendix. The representative diagrams may be found in Fig. 5. We also proposed a possible extension of the derived fourth-order contributions to all orders of perturbation theory.

The derived expressions may be useful for an analysis of the completeness of all-order methods in the fourth order of perturbation theory and for designs of next-generation approximations in atomic many-body calculations.

### Acknowledgments

We would like to thank Sergey Porsev for comments on the manuscript. This work was supported in part by the National Science Foundation.

### APPENDIX A: FOURTH-ORDER CORRECTIONS TO MATRIX ELEMENTS

Here we tabulate fourth-order corrections to matrix elements of one-particle operator involving triple excitations and nonlinear contribution from double excitations. The classification of the diagrams and notation were introduced in the main text of the paper. Briefly, the matrix elements  $g_{ijkl}$  of the Coulomb interaction are defined by Eq. (5). The quantities  $\tilde{g}_{ijkl}$  are antisymmetric combinations  $\tilde{g}_{ijkl} = g_{ijkl} - g_{ijlk}$ . Matrix elements of a non-scalar one-particle operator  $Z$  are denoted as  $z_{ij}$ . Core orbitals are enumerated by letters  $a, b, c, d$ , complementary excited states are labelled by  $m, n, r, s$ , and valence orbitals are denoted by  $v$  and  $w$ . The notation  $\varepsilon_{xy\dots z}$  stands for  $\varepsilon_x + \varepsilon_y + \dots + \varepsilon_z$ . The terms denoted *c.c.*

are to be calculated by taking the hermitian conjugate of all preceding contributions and swapping labels  $v$  and  $w$ .

For convenience of drawing the graphs, the sequence of interactions in numerators is sorted so that the interaction to the right of another interaction appears lower in the corresponding Brueckner-Goldstone diagram.

$$\begin{aligned}
 Z_{1 \times 2}(T_c) = & \sum_{abcmnr} \frac{\tilde{g}_{abnr} z_{cv} g_{nr cm} g_{mwab}}{(\varepsilon_{mw} - \varepsilon_{ab})(\varepsilon_{nr} - \varepsilon_{ab})(\varepsilon_{nrw} - \varepsilon_{abc})} + \\
 & \sum_{abcmnr} \frac{\tilde{g}_{abnr} z_{cv} \tilde{g}_{rwcm} g_{mnab}}{(\varepsilon_{mn} - \varepsilon_{ab})(\varepsilon_{nr} - \varepsilon_{ab})(\varepsilon_{nrw} - \varepsilon_{abc})} + \\
 & - \sum_{abcmnr} \frac{\tilde{g}_{abnr} z_{cr} \tilde{g}_{rwcm} g_{mnab}}{(\varepsilon_{mn} - \varepsilon_{ab})(\varepsilon_{nv} - \varepsilon_{ab})(\varepsilon_{nrw} - \varepsilon_{abc})} + \\
 & \sum_{abcmnr} \frac{\tilde{g}_{abrv} z_{cn} \tilde{g}_{nr cm} g_{mwab}}{(\varepsilon_{mw} - \varepsilon_{ab})(\varepsilon_{rv} - \varepsilon_{ab})(\varepsilon_{nrw} - \varepsilon_{abc})} + \\
 & \sum_{abcmnr} \frac{\tilde{g}_{abrv} z_{cn} \tilde{g}_{rwcm} g_{mnab}}{(\varepsilon_{mn} - \varepsilon_{ab})(\varepsilon_{rv} - \varepsilon_{ab})(\varepsilon_{nrw} - \varepsilon_{abc})} + \\
 & \sum_{abcmnr} \frac{\tilde{g}_{bcnr} z_{av} g_{nr cm} \tilde{g}_{mwab}}{(\varepsilon_{mw} - \varepsilon_{ab})(\varepsilon_{nr} - \varepsilon_{bc})(\varepsilon_{nrw} - \varepsilon_{abc})} + \\
 & \sum_{abcmnr} \frac{\tilde{g}_{bcnr} z_{av} \tilde{g}_{rwcm} \tilde{g}_{mnab}}{(\varepsilon_{mn} - \varepsilon_{ab})(\varepsilon_{nr} - \varepsilon_{bc})(\varepsilon_{nrw} - \varepsilon_{abc})} + \\
 & - \sum_{abcmnr} \frac{\tilde{g}_{bcnv} z_{ar} \tilde{g}_{rwcm} \tilde{g}_{mnab}}{(\varepsilon_{mn} - \varepsilon_{ab})(\varepsilon_{nv} - \varepsilon_{bc})(\varepsilon_{nrw} - \varepsilon_{abc})} + \\
 & \sum_{abcmnr} \frac{\tilde{g}_{bcrv} z_{an} \tilde{g}_{nr cm} \tilde{g}_{mwab}}{(\varepsilon_{mw} - \varepsilon_{ab})(\varepsilon_{rv} - \varepsilon_{bc})(\varepsilon_{nrw} - \varepsilon_{abc})} + \\
 & \sum_{abcmnr} \frac{\tilde{g}_{bcrv} z_{an} \tilde{g}_{rwcm} \tilde{g}_{mnab}}{(\varepsilon_{mn} - \varepsilon_{ab})(\varepsilon_{rv} - \varepsilon_{bc})(\varepsilon_{nrw} - \varepsilon_{abc})} + \\
 & \sum_{abcdmn} \frac{\tilde{g}_{bdmn} z_{cv} \tilde{g}_{ancd} \tilde{g}_{mwab}}{(\varepsilon_{mn} - \varepsilon_{bd})(\varepsilon_{mw} - \varepsilon_{ab})(\varepsilon_{mnw} - \varepsilon_{bcd})} + \\
 & - \sum_{abcdmn} \frac{\tilde{g}_{bdmn} z_{cv} \tilde{g}_{awcd} g_{mnab}}{(\varepsilon_{mn} - \varepsilon_{ab})(\varepsilon_{mn} - \varepsilon_{bd})(\varepsilon_{mnw} - \varepsilon_{bcd})} + \\
 & - \sum_{abcdmn} \frac{\tilde{g}_{bdmv} z_{cn} \tilde{g}_{ancd} \tilde{g}_{mwab}}{(\varepsilon_{mv} - \varepsilon_{bd})(\varepsilon_{mw} - \varepsilon_{ab})(\varepsilon_{mnw} - \varepsilon_{bcd})} + \\
 & \sum_{abcdmn} \frac{\tilde{g}_{bdnv} z_{cm} \tilde{g}_{ancd} \tilde{g}_{mwab}}{(\varepsilon_{mw} - \varepsilon_{ab})(\varepsilon_{nv} - \varepsilon_{bd})(\varepsilon_{mnw} - \varepsilon_{bcd})} + \\
 & - \sum_{abcdmn} \frac{\tilde{g}_{bdnv} z_{cm} \tilde{g}_{awcd} \tilde{g}_{mnab}}{(\varepsilon_{mn} - \varepsilon_{ab})(\varepsilon_{nv} - \varepsilon_{bd})(\varepsilon_{mnw} - \varepsilon_{bcd})} + \\
 & - \sum_{abcdmn} \frac{\tilde{g}_{cdmn} z_{bv} g_{ancd} \tilde{g}_{mwab}}{(\varepsilon_{mn} - \varepsilon_{cd})(\varepsilon_{mw} - \varepsilon_{ab})(\varepsilon_{mnw} - \varepsilon_{bcd})} + \\
 & \sum_{abcdmn} \frac{\tilde{g}_{cdmn} z_{bv} \tilde{g}_{awcd} g_{mnab}}{(\varepsilon_{mn} - \varepsilon_{ab})(\varepsilon_{mn} - \varepsilon_{cd})(\varepsilon_{mnw} - \varepsilon_{bcd})} + \\
 & \sum_{abcdmn} \frac{\tilde{g}_{cdmv} z_{bn} g_{ancd} \tilde{g}_{mwab}}{(\varepsilon_{mv} - \varepsilon_{cd})(\varepsilon_{mw} - \varepsilon_{ab})(\varepsilon_{mnw} - \varepsilon_{bcd})} +
 \end{aligned}$$









$$\sum_{abcmnr} \frac{z_{br} \tilde{g}_{acmn} \tilde{g}_{rwc} g_{mnab}}{(\varepsilon_{mn} - \varepsilon_{ab})(\varepsilon_{rw} - \varepsilon_{bv})(\varepsilon_{rw} - \varepsilon_{cv})} + c.c.$$

Finally, the normalization correction due to valence triple excitations is defined as

$$Z_{\text{norm}}(T_v) = -\frac{1}{2} \left( N_v^{(3)}(T_v) + N_w^{(3)}(T_v) \right) z_{vw}.$$

The correction to normalization may be represented as (the terms denoted *c.c.* are to be calculated by taking the hermitian conjugate of all preceding contributions)

$$N_v^{(3)}(T_v) = \sum_{abcmnr} \frac{\tilde{g}_{abnr} g_{nr} g_{mvab}}{(\varepsilon_{mv} - \varepsilon_{ab})(\varepsilon_{nr} - \varepsilon_{ab})^2} + \sum_{abcmn} \frac{\tilde{g}_{bcmn} \tilde{g}_{ancv} \tilde{g}_{mvab}}{(\varepsilon_{mn} - \varepsilon_{bc})^2 (\varepsilon_{mv} - \varepsilon_{ab})} +$$

$$\begin{aligned} & \sum_{abmnr} \frac{\tilde{g}_{abnr} g_{nr} g_{bm} \tilde{g}_{mvav}}{(\varepsilon_m - \varepsilon_a)(\varepsilon_{nr} - \varepsilon_{ab})^2} + \\ & \sum_{abcmn} \frac{\tilde{g}_{bcmn} g_{anbc} \tilde{g}_{mvav}}{(\varepsilon_m - \varepsilon_a)(\varepsilon_{mn} - \varepsilon_{bc})^2} + \\ & \sum_{abmnr} \frac{\tilde{g}_{abnr} \tilde{g}_{rvbm} \tilde{g}_{mnab}}{(\varepsilon_{mn} - \varepsilon_{av})(\varepsilon_{nr} - \varepsilon_{ab})^2} + \\ & \sum_{abmnr} \frac{\tilde{g}_{abnr} \tilde{g}_{rvbm} g_{mnab}}{(\varepsilon_{mn} - \varepsilon_{ab})(\varepsilon_{nr} - \varepsilon_{ab})^2} + \\ & - \sum_{abcmn} \frac{\tilde{g}_{bcmn} g_{avbc} g_{mnab}}{(\varepsilon_{mn} - \varepsilon_{av})(\varepsilon_{mn} - \varepsilon_{bc})^2} + \\ & - \sum_{abcmn} \frac{\tilde{g}_{bcmn} \tilde{g}_{avcv} g_{mnab}}{(\varepsilon_{mn} - \varepsilon_{ab})(\varepsilon_{mn} - \varepsilon_{bc})^2} + c.c. \end{aligned}$$

- 
- [1] C. S. Wood, S. C. Bennett, D. Cho, B. P. Masterson, J. L. Roberts, C. E. Tanner, and C. E. Wieman, *Science* **275**, 1759 (1997).
  - [2] S. C. Bennett and C. E. Wieman, *Phys. Rev. Lett.* **82**, 2484 (1999).
  - [3] A. Derevianko, *Phys. Rev. Lett.* **85**, 1618 (2000); V. A. Dzuba *et al.*, *Phys. Rev. A* **63**, 044103 (2001); M. G. Kozlov *et al.*, *Phys. Rev. Lett.* **86**, 3260 (2001); W. R. Johnson *et al.*, *Phys. Rev. Lett.* **87**, 233001 (2001); A. I. Milstein and O. P. Sushkov, e-print: hep-ph/0109257; A. Derevianko, *Phys. Rev. A* **65**, 012106 (2002); Dzuba *et al.*, e-print: hep-ph/0111019.
  - [4] V. A. Dzuba, V. V. Flambaum, and O. P. Sushkov, *Phys. Lett. A* **141**, 147 (1989).
  - [5] S. A. Blundell, W. R. Johnson, and J. Sapirstein, *Phys. Rev. Lett.* **65**, 1411 (1990), *Phys. Rev. D* **45**, 1602 (1992).
  - [6] M. Y. Amusia and N. A. Cherepkov, *Case Studies in Atomic Physics* **5**, 47 (1975).
  - [7] J. Sapirstein, *Rev. Mod. Phys.* **70**, 55 (1998).
  - [8] W. R. Johnson, Z. W. Liu, and J. Sapirstein, *At. Data Nucl. Data Tables* **64**, 279 (1996).
  - [9] J. Čížek, *J. Chem. Phys.* **45**, 4256 (1966).
  - [10] F. Coester and H. G. Kümmer, *Nucl. Phys.* **17**, 477 (1960).
  - [11] I. Lindgren and J. Morrison, *Atomic Many-Body Theory* (Springer-Verlag, Berlin, 1986), 2nd ed.
  - [12] S. A. Blundell, W. R. Johnson, Z. W. Liu, and J. Sapirstein, *Phys. Rev. A* **40**, 2233 (1989).
  - [13] S. A. Blundell, W. R. Johnson, and J. Sapirstein, *Phys. Rev. A* **43**, 3407 (1991).
  - [14] M. S. Safronova, W. R. Johnson, and A. Derevianko, *Phys. Rev. A* **60**, 4476 (1999).
  - [15] S. A. Blundell, D. S. Guo, W. R. Johnson, and J. Sapirstein, *At. Data Nucl. Data Tables* **37**, 103 (1987).
  - [16] S. Wolfram, *The Mathematica Book* (Wolfram Media/Cambridge University Press, Champaign, Illinois, 1999), 4th ed.
  - [17] R. F. Bishop and H. G. Kümmer, *Physics Today* **3**, 52 (1987).
  - [18] M. S. Safronova, A. Derevianko, and W. R. Johnson, *Phys. Rev. A* **58**, 1016 (1998).